SAND REPORT

SAND2002-2744
Unlimited Release
Printed November 2002

Design for an Internal Circular Compression Band Restraint Device (Marman Clamp, V-Band)

Paul R. Klarer, Mark R. Vaughn, Jennifer F. Gilbride, Roy S. Baty, and Jerry L. Adams

Prepared by
Sandia National Laboratories
Albuquerque, New Mexico 87185 and Livermore, California 94550

Sandia is a multiprogram laboratory operated by Sandia Corporation,
a Lockheed Martin Company, for the United States Department of Energy's
National Nuclear Security Administration under Contract DE-AC04-94-AL85000.

Sandia National Laboratories

Issued by Sandia National Laboratories, operated for the United States Department of Energy by Sandia Corporation.

Printed in the United States of America. This report has been reproduced directly from the best available copy.

Available to DOE and DOE contractors from
U.S. Department of Energy
Office of Scientific and Technical Information
P.O. Box 62
Oak Ridge, TN 37831

Telephone: (865)576-8401
Facsimile: (865)576-5728
E-Mail: reports@adonis.osti.gov
Online ordering: http://www.doe.gov/bridge

Available to the public from
U.S. Department of Commerce
National Technical Information Service
5285 Port Royal Rd
Springfield, VA 22161

Telephone: (800)553-6847
Facsimile: (703)605-6900
E-Mail: orders@ntis.fedworld.gov
Online order: http://www.ntis.gov/help/ordermethods.asp?loc=7-4-0#online

SAND2002-2744J
Unlimited Release
Printed November 2002

Design for an Internal Circular Compression Band Restraint Device (Marman Clamp, V-Band)

Paul R. Klarer, P.E.
Mark R. Vaughn, Ph.D.
Roy S. Baty, Ph.D.
Jennifer F. Gilbride
Jerry L. Adams

Sandia National Laboratories
Albuquerque, New Mexico USA

Keywords: *v-band, internal circular compression restraint, Marman Clamp, applied Finite Element Analysis*

Abstract

An application requirement is addressed that does not allow a conventional external v-band to be used. An internal v-band design was done which satisfies the performance requirements. This report describes that design and the results of the analysis. The desired result of this analysis is to verify that the v-band will not fail under the applied load, the v-band is not self-locking and therefore fail to release when desired, the required expansion force is not greater than a specified limit, and that the natural vibration modes and frequencies do not present any anticipated problems (such as resonance and/or mode coupling) in the application. A successful design is illustrated using the output from a Finite Element Analysis. A sensitivity analysis indicates the importance and interrelationships between several key design parameters, a result that tends to agree with many years of v-band design experience at Sandia National Laboratories.

Introduction

A requirement for a cylindrical mechanical coupling device can easily be fulfilled with a conventional circular compression band restraint, typically termed a 'v-band'. The v-band coupling technique is well understood for coaxial cylinders butted end-to-end. In the past this has typically been accomplished by providing a pair of matched engagement flanges on the outer surface of the cylinders[1,2] and coupling the cylinders together using the engagement flanges and a circular compression band installed as shown in Figure 1. Note the flanges and the v-band incorporate angled contact faces that translate a portion of the radial compression force into an axial force to effectively preload the butt joint.

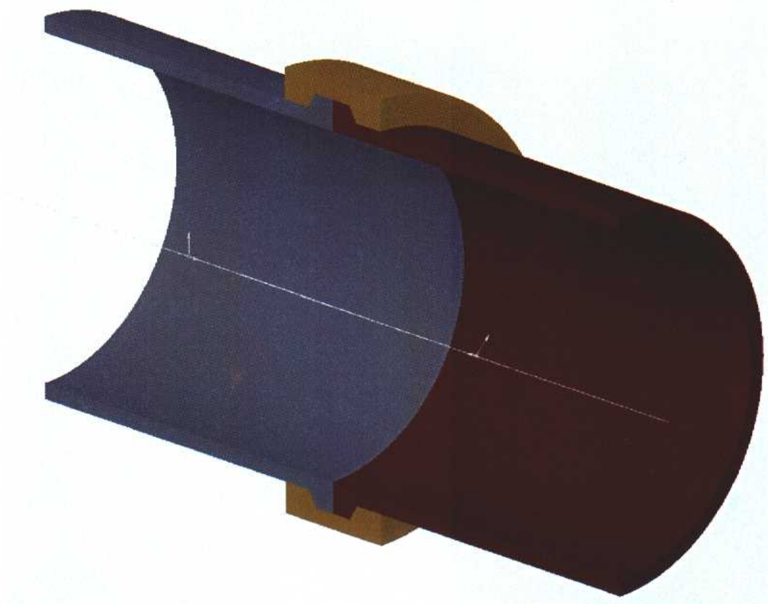

Figure 1. A typical external v-band installation

An application requirement for a v-band design was presented that did not allow conventional external v-band use, for a variety of reasons. An alternative internal v-band design was proposed which would satisfy the performance requirements. This report describes that design and the results of the analysis. The v-band is intended to be inserted inside a pair of cylindrical mating parts butted together end-to-end to provide a robust, decoupling mechanical joint, as shown in Figure 2.

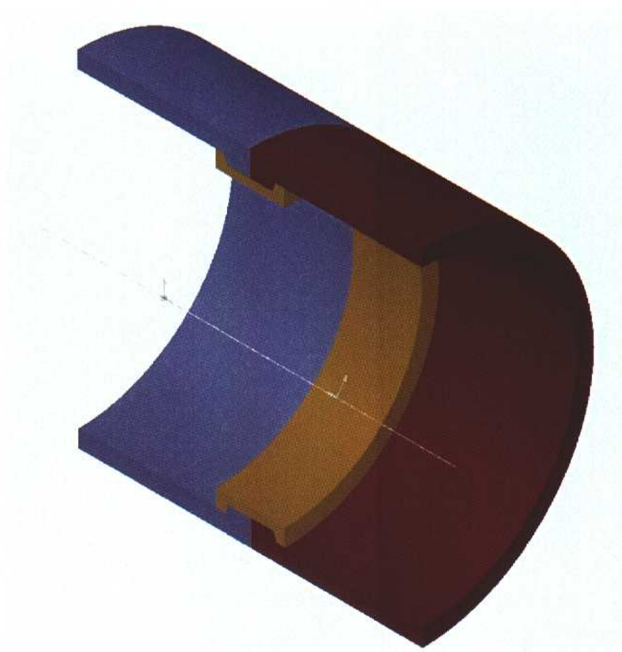

Figure 2. A generic internal v-band installation

Note the actual v-band is fabricated in the 'released' shape illustrated in Figure 3. An expansion device (such as a bolt, turnbuckle, or spreader) is applied along a chord of the v-band's basically circular shape between the two 'ears' in order to radially expand the v-band to its installed shape and bring the two ramped surfaces into contact with mating ramps located on the inner diameter of the mating cylindrical parts. This is analogous to the action of a conventional snap ring, the difference being that although the v-band is an internally mounted device, its normal 'un-deflected' shape is fully retracted, as opposed to fully expanded as an internal snap ring would be.

Because the v-band is fabricated as shown, it will naturally resume the shape illustrated in Figure 3 whenever the expansion device between the ears is relaxed or removed, as long as it is not stressed beyond yield. A major simplifying assumption, for the purposes of examining the v-band, is to assume the two joined cylinders do not significantly flex or distort their shape when in loaded contact with the v-band. Figure 3 shows the v-band and the planes of symmetry assumed, for purposes of simplifying the stress analysis.

Figure 3. Internal V-band with planes of symmetry shown.

Figure 4 shows the portion of the v-band that remains after simplification by symmetry. Important design constraints include the required expansion force to achieve full deflection of the v-band to its final shape, maximum allowable stress in the material, and the loads imposed on the v-band by the application of tensile forces along the axis of the cylinders, which will tend to separate the mating parts from each other along the main longitudinal axis at the butt joint. The desired result of this analysis is to verify that the v-band will not fail under the applied load, the v-band is not self-locking and therefore fail to release when desired, the required expansion force is not greater than a specified limit, and that the natural vibration modes and frequencies do not present any anticipated problems (such as resonance and/or mode coupling) in the application. The forces used in the analysis are shown as magenta arrows and the constraints on the body are shown as green arrows with perpendicular 'tails' at the ends.

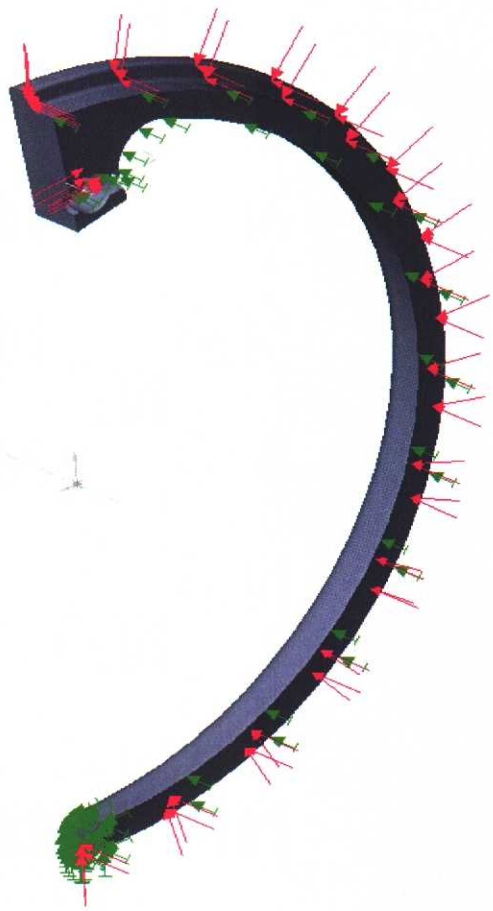

Figure 4. V-Band after cutting along planes of symmetry. Forces are shown in magenta and constraints in green

Analysis

The imposed loads on the system include two forces; a constant force **Ft** of $1.1*10^3$ kN (250,000 lb_f) applied to one cylinder along its axis (with the other cylinder held fixed) thereby placing the cylinder in tension, and a force **Fs** applied to the spreader ears, representing a spreading device to expand the v-band radially. The mandatory conditions for a successful v-band design are:

- The spreader force **Fs** may not exceed 33.4 kN (7500 lb_f), to avoid failure of the spreader mechanism (external to the v-band itself).
- The v-band material itself (AISI 4340 Q&T fully hard) must not fail due to **Ft**

- The ramp angle of the v-band must be large enough to ensure it is not self-locking with the mating surfaces on the two cylinders when the axial load is applied.

For the purposes of this analysis, the spreader mechanism was represented by a 6.35 mm (¼") diameter rod. Questions of interest for the purpose of analysis included:

- What is the 'optimal' cross section configuration of the v-band to maximize flexibility, minimize the force on the bolt, and still remain below the material's yield stress level when all loads are applied?
- What is the minimum required ramp angle to ensure the v-band will not be self-locking when the spreader bolt is removed or released?
- How much force on the spreader bolt is required to expand the v-band into position when initially installed?
- How much total force is imposed on the spreader bolt when the maximum $1.1*10^3$ kN (250,000 lb_f) axial load is applied to the cylinder and transferred to the installed (expanded) v-band?
- Will the spreader bolt fail when the axial load is applied?
- Will the v-band itself fail when the axial load is applied?

In answering the above questions of interest, the first two in the list necessarily make the analysis process an iterative one. After determining the absolute minimum ramp angle to ensure the v-band will release properly, one must then calculate the forces required for equilibrium without violating the maximum force on the bolt, apply them to the model, and then determine if the v-band material is subject to stress failure. If not, the model's stress plot is examined to determine where 'excess' material exists and the model is then 'trimmed' to remove it. This results in a change in the flexible characteristics of the model. Consequently, a new set of forces must be determined for equilibrium and the process repeats. This sequence is followed until a point is reached where one of the conditions fail. In general (for v-bands), while a larger ramp angle, α, reduces the chances of self-locking, it simultaneously increases the radial component of the imposed forces and results in increased force on the spreader bolt. Thinning of the v-band cross section tends to reduce the forces that resist the bolt's work of expanding the v-band into the installed position, thereby reducing the magnitude of the radial components in the force system.

Due to the conical geometry of the v-band's contact surfaces (the angled ramp in three dimensions is in fact a cone), an analysis of the system by conventional manual means appeared to be complex and problematic. A further consideration was that since a major design goal was to find an optimum configuration with minimal material, an iterative design and analysis process would be required. It was therefore determined that a numerical analysis using available Finite Element Analysis (FEA) tools would be advantageous, enabling exploration of a range of solutions in a relatively short time.

For the purposes of an FEA analysis, the model was constrained along the planes of symmetry as follows:

- The surface exposed by the symmetry plane identified in Figure 3 as Plane 4 was not allowed to translate along any vector normal to Plane 4, that vector being the major cylindrical axis of the v-band.

- The surface exposed by the symmetry plane identified in Figure 3 as Plane 5 was not allowed to translate in any direction described by a vector lying in Plane 5.

These constraints allowed the v-band to freely expand radially as a result of the imposed loading.

Description of Force System

The cross section shown in Figure 5 illustrates a small differential area (dA) located on the angled face of the v-band ramp. This face is the pressure-bearing surface of contact between the v-band and the two cylinders being mated, as illustrated in Figure 2. The loading forces applied to the v-band axially and radially combine to produce a net pressure on this dA, which must be integrated to find the total force on the v-band's ramp face. Because the v-band axis is asymmetrical, due to the spreader ears and the conical surface of the ramp face, formulation of the complete symbolic integral for total force on the ramp face is problematic. Instead, a simpler force representation was used to obtain the radial and axial force components, which were then fed into a numerical finite element model for solving.

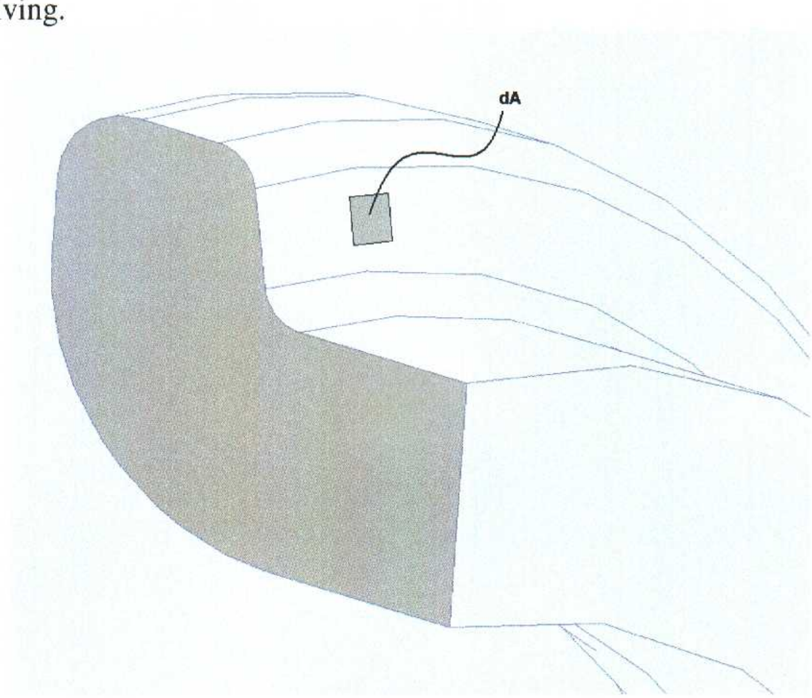

Figure 5. Cross section of V-Band with loaded differential area shown

The cross section of the modeled ¼ section in Figure 6 shows the angled ramp and the forces present as a result of the applied tensile load, **Ft**. The normal force, **N**, depends on the ramp angle. The frictional force, **Ff**, depends on the ramp angle, the normal force **N**, and the coefficient of friction of the ramp surface with its mating surface on the mating part (not shown). The planes of symmetry in Figure 3 correspond to both the indicated plane of symmetry and the viewing plane in Figure 6. Figure 4 shows the v-band after splitting it along the two planes of symmetry, applying restraints to the planes of symmetry (green arrows), and applying forces (magenta arrows) to the expansion ear and the angled ramp. These are the conditions under which the FEA simulations were conducted. Note that the forces on the ramp shown in Figure 4 are given as radial and axial components rather than as a force system normal to the conical ramp face. This greatly facilitated the computation of the forces required for equilibrium by allowing the spreader bolt force **Fs** to be computed to account only for the radial components of both **N** and **Ff**.

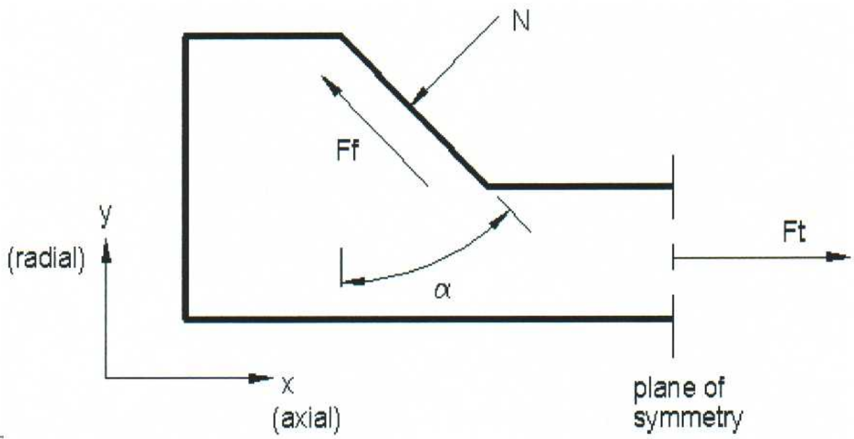

Figure 6. Cross section of V-Band with forces shown

Starting with a thin slice exposing the cross section of the v-band as shown in Figure 6, the overall force system in a 2D representation is derived as follows, assuming a very small notional area on the ramped contact face of the v-band.

The normal force **N** on the ramp face results from the applied tensile force **Ft**

$$N := \frac{Ft}{\cos(\alpha)}$$ **Equation 1**

The radial component of normal force **N** depends on the ramp angle α

$$Fr := N \cdot \sin(\alpha)$$ **Equation 2**

The frictional force **Ff** along ramp face depends on **N** and μ

$$Ff := \mu \cdot N$$ **Equation 3**

Then the axial and radial components of the frictional force can be expressed as

$$Ffx := Ff \cdot \sin(\alpha)$$ **Equation 4**

$$Ffy := Ff \cdot \cos(\alpha)$$ **Equation 5**

Summing the forces in X (axial direction) the net axial force on the ramped face is obtained:

$$Fx := Ffx + Ft$$ **Equation 6**

Summing the forces in Y (radial direction) the net radial force on the ramped face is obtained:

$Fy := Ffy - Fr$ **Equation 7**

Equation 6 and 7 provide the net axial and radial forces present on the v-band's ramped contact face over a notionally very small area. Determining the total integral value of the axial and radial components on the fully 3D v-band object can be accomplished using integration techniques or by using a 3D Finite Element Analysis (FEA) tool. Because of the v-band's spreader ears, obtaining an accurate closed form expression for the integration of the forces on the differential area leads to a host of practical issues making such an approach problematic. Rather, an FEA technique was employed due to its ease of use and greater facility for visualizing the results of the computations. The use of FEA also greatly facilitated running a series of cases involving geometry and force system changes to obtain an efficient v-band design.

Procedure

Note that the ramp interface between the v-band and the two mating cylinders will become self locking when the radial component of the frictional force equals or exceeds the radial component of the normal force, such that the normal force cannot overcome the friction keeping the v-band in place:

self-locking @ Ffy >= Fr

Therefore, in order to ensure the system is NOT self-locking and will ALWAYS release, the minimum ramp angle must satisfy the condition:

$\boldsymbol{\alpha > \arctan(\mu)}$

In addition, the ramp surface must not incur any galling, so it is imperative that it be sufficiently hardened and lubricated with a dry lubricant such as molybdenum disulfide. These two assumptions were made in order to disregard the ramp's surface condition while performing the analysis.

After applying a force to emulate the expansion device spreading the expansion ears apart and forcing the v-band to the desired size, the v-band was loaded in tension along its major longitudinal axis and then examined for predicted stress failure. Because the conditions for equilibrium require that the spreader bolt oppose the net radial forces on the ramped face, a critical design check was required to ensure the force on the bolt did not exceed the maximum allowed value of 33.4 kN (7500 lb_f).

Variable design parameters during the analysis and simulation process included the ramp angle, the v-band cross-section profile, and the coefficient of friction on the ramp surface. The results of the simulations provided the stress plots shown in the next section, as well as predicted deflection plots. The predicted deflection plots were used to predict the force required to expand the v-band into position against its mating parts.

Stress Results

Multiple iterations of the cross-section design, which included various values for the coefficient of friction μ on the angled ramp and for the ramp angle α, resulted in a configuration wherein the cross section appeared to be as small and thin as possible, while still satisfying the design failure criteria. Figure 7 shows the resulting v-band design under load, and highlights the area of stress that is above the allowable yield stress in red. All blue regions are at a level of stress that is less than the yield stress, so are not at risk of failure.

Figure 7. Factor Of Safety plot. Red area is stressed above yield for the material.

Figure 8 shows the VonMises stress distribution in the v-band, clearly illustrating the remainder of the part is well within the maximum allowable stress level for the material (approximately 1.38 GPa or 200,000 psi).

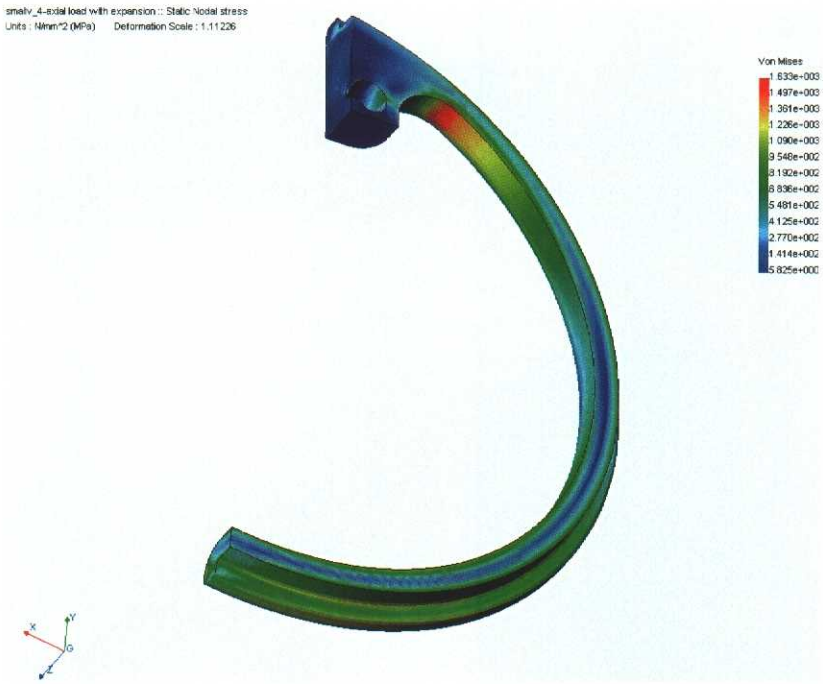

Figure 8. Stress plot of v-band under load.

Figure 9. Yielding area in cross section, yield stress level is colored red

Figure 9 illustrates the predicted area of failure in cross section, showing that the actual material that will fail does not penetrate to a significant depth through the part but is limited to a region very near the surface. It is reasonable to assume that a relatively minor change to the v-band design at the area of maximum stress should alleviate this issue.

Note the red areas at the root of the ramp face in Figure 10 indicate the material has been stressed beyond the yield point. The section view in Figure 10 shows this to be a superficial effect. Note also in Figure 10 that the original undeflected profile is shown as a red outline.

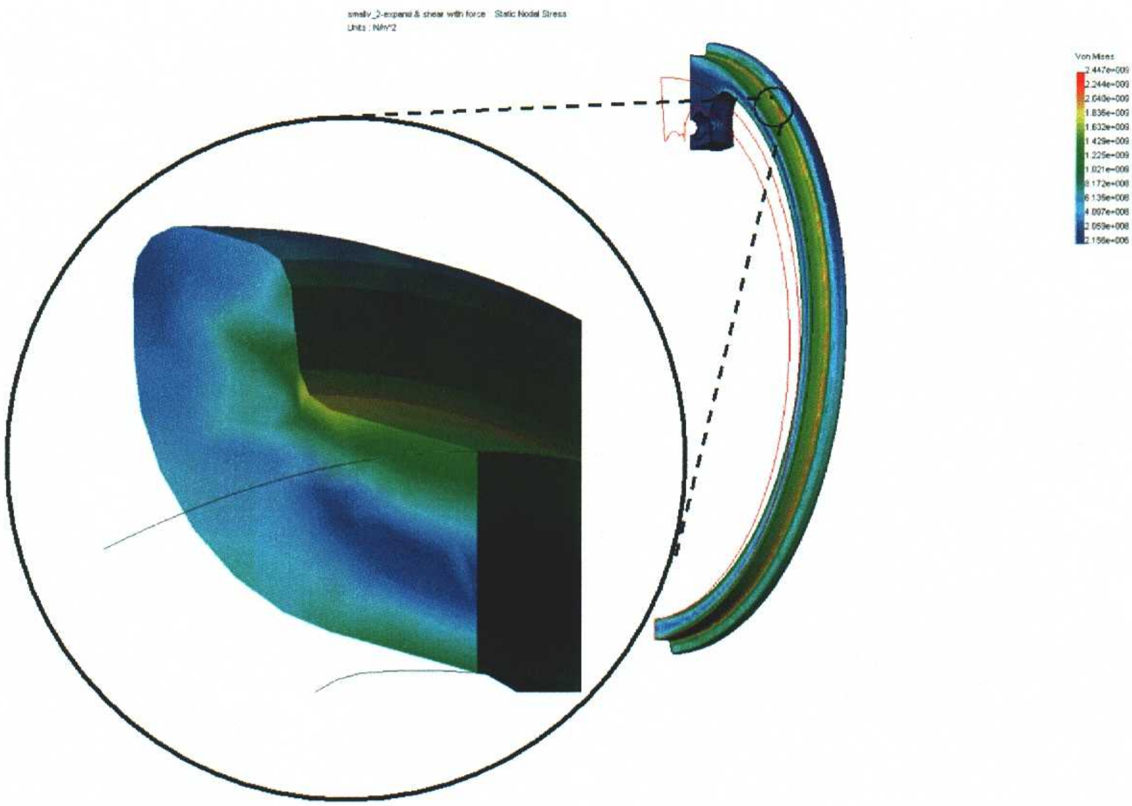

Figure 10. Stress plot with detail section of ramp root area

The yellow region in the detail section in Figure 10 represents the material stressed beyond the yield point; the green and blue regions represent material that is still within the elastic region below the yield point. This shows that although the surface material may yield, the overwhelming majority of the material will not yield and therefore the effect on material strength and permanent deformation of the part will be minimal.

To date, analysis shows that the following conditions are true for the existing design, where the ramp angle is assumed to be 10 degrees and the coefficient of friction is assumed to be 0.065:

- The v-band expansion bolt requires approximately 1780 N (400 lb_f) of force (axial) to expand the v-band into the installed position
- The bolt experiences approximately 24 kN (5400 lb_f) of force (axial) when the $1.1*10^3$ kN (250,000 lb_f) axial load is applied
- The bolt (4130 Q&T to 36-38 Rockwell C) will yield at approximately 33.4 kN (7500 lb_f) axially, so the bolt has a worst case safety factor of ~1.4

- There are small spots on the v-band at the root of the angled ramp that appear to be approaching yield, however they do not penetrate the cross section to any significant degree and so are only surface effects
- The v-band stress and Factor of Safety simulation results indicate that there is a small area in the v-band adjacent to the expansion ear that experiences some yielding at the surface. However, the remainder of the v-band has a safety factor of greater than or equal to1

Frequency Analysis

For the purposes of a frequency analysis, one of the planes of symmetry was eliminated so the stiffness of the entire v-band cross section would be included. Figure 11 and Figure 12 show the first two vibration modes and natural frequencies of the v-band. Note the first and second modal frequencies differ only by ~3%, and the third mode was found to occur at approximately 217Hz, a result far enough removed from the first two modes as to render it not significant as a source of concern. The closeness of the first two modal frequencies could be an important design issue and is recommended for further study.

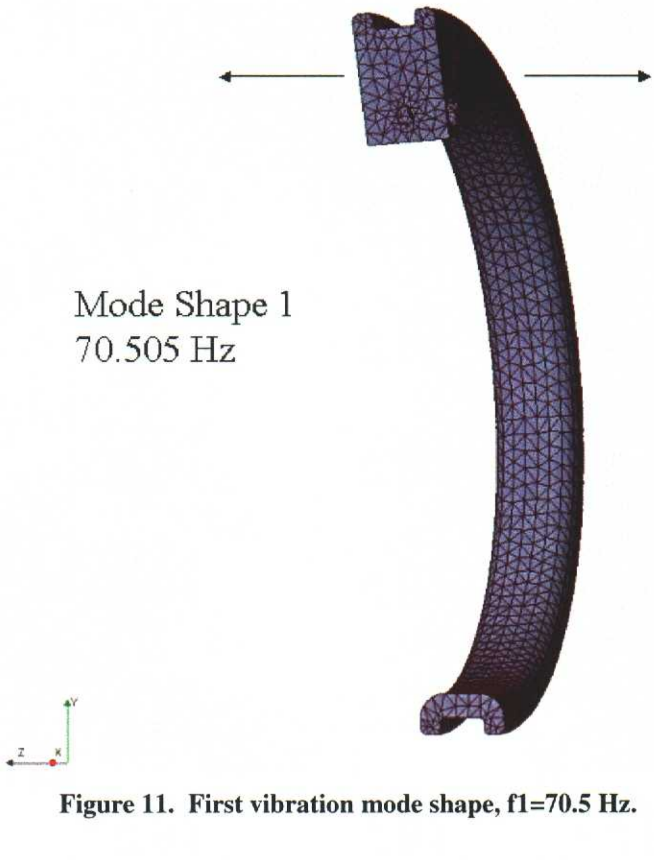

Figure 11. First vibration mode shape, f1=70.5 Hz.

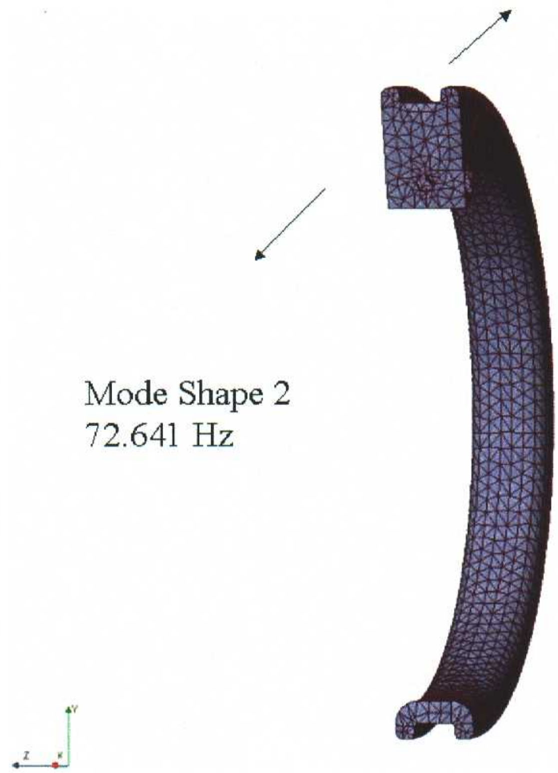

Figure 12. Second vibration mode shape, f2=72.641 Hz.

Conclusions

The v-band design, as it currently exists, should perform without failure due to the imposed loads as they are currently specified. Although there is an indication of possible yielding in an area immediately adjacent to the expansion ear feature, it does not appear to be a major defect. In order to eliminate this possible source of failure, a minor modification to that area's cross section may be required.

Note that the original v-band part model required significant changes in order to optimize its stiffness and stress distribution to satisfy all design parameters. The potential for interaction of the first two vibration modes should be investigated in the context of the application to determine if in fact this is a serious area of concern, and modifications made to the v-band design to force frequency separation of those two modes. To date, the two mating cylindrical rings have not been analyzed. They are expected to outperform the v-band since they are thicker in cross section, they are continuous in cross section about the major axis, and are of the same material as the v-band.

It should also be noted that the v-band's performance is highly dependent on three parameters: the coefficient of friction, μ, on the ramp surface with respect to the mating rings, the ramp angle, α, and the applied tensile load, Ft. A sensitivity analysis shows the net force in the radial direction depends on the applied force times the difference between the coefficient of friction and the tangent of the ramp angle. Within the limited range of interest, the relationship appears to be nearly linear and highly sensitive to both μ and α, primarily because the ramp angle can be small and the tangent of the angle changes very quickly, i.e., the slope of the tangent function approaches infinity as the angle approaches zero.

$$Fnet = Ft(\tan(\alpha) - \mu)$$

Accordingly, the radial forces resulting from the applied load through the ramp angle can vary by two orders of magnitude as the ramp angle changes for values of α between ~4 and ~8 degrees. Holding the ramp angle α to a high manufacturing tolerance will be essential at these small values of α, to ensure this variable is tightly controlled. The coefficient of friction is a parameter that is very difficult to control with any precision, so this variable poses significant implementation issues. A very specific material surface condition (hardness and finish) must be achieved during fabrication, and consistent use of dry lubricant during assembly must be implemented in order to hold μ to within a narrow range.

It is interesting to note that due to the loading geometry, as the coefficient of friction on the ramp surface increases, the imposed radial load and subsequent compression load on the expansion bolt actually *decreases*, since friction on the ramp acts in the same direction as the forces exerted by the expansion bolt. This indicates that the coefficient of friction on the ramp's surface is not a critical parameter, particularly if the ramp angle is greater than or equal to approximately 10 degrees. This value corresponds to empirical results developed over many years of external v-band design and testing at Sandia National Laboratories.

Acknowledgements

Sandia is a multiprogram laboratory operated by Sandia Corporation, a Lockheed Martin Company, for the United States Department of Energy under Contract DE-AC04-94AL85000.

References

1. "New Considerations to the Design and Calculation Methods of Large Diameter Marman Clamp Band Connection Systems", W. Huessler, IAF '86: 37th Congress of the International Astronautical Federation, Innsbruck, Austria, October 4-11, 1986 : Space, New Opportunities for All People.

2. "Nonlinear Finite Element Evaluation of Marman Clamp Structural Capability", R, DiTolla and M. Ernst; 35th AIAA/ASME/ASCE/AHS/ASC Structures, Structural Dynamics, and Materials Conference, April 18-20, 1994, Hilton Head, SC, USA

DISTRIBUTION:

2	MS 0482	R. Baty, 02131
5	MS 0482	J. Martinez, 02131
1	MS 0482	K. Meeks, 02131
1	MS 0429	S. Rottler, 02100
1	MS 1125	P. Klarer, 15252
1	MS 1125	M. Vaughn, 15252
1	MS 1125	J. Gilbride, 15252
1	MS 1125	K. Miller, 15252
1	MS 1002	S. Roehrig, 15200
1	MS 0627	J. Adams, 02991
1	MS 0627	L. Grube, 02991
1	MS 9018	Central Technical Files, 8945-1
2	MS 0899	Technical Library, 9616
1	MS 0612	Review & Approval Desk, 9612 For DOE/OSTI
1	MS 1004	D. Miller, 15221